Characterization of Silicon Thin Films for Novel Applications in Renewable Energy

Dylan Bilek, Muskaan Kanoi, Jesus Reyes, Valeria Rodriguez, Dylan Voss

UCDAVIS MATERIALS SCIENCE AND ENGINEERING

Team Station 112

Solar Light Technologies

Motivation

Crystalline silicon solar cells currently dominate the photovoltaic market, accounting for approximately 90% of the market share due to their high efficiencies [1]. However, their heavy and inflexible nature presents challenges when it comes to mounting them. Our sponsor's objective, PI Energy, is to develop a flexible photovoltaic that can be mounted on various surfaces.

The goal of our project was to investigate how different laser annealing and processing conditions of the seed layer would impact the epitaxial growth of these solar cells, which in turn affects the efficiency. Our group analyzed the surface roughness, morphology, and recombination characteristics of PI Energy's photovoltaics under various processing conditions.

Introduction

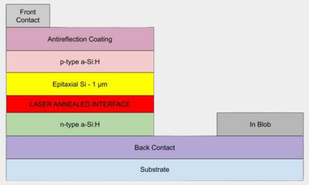

Fig 1. PI Energy's solar cell. It is a p-i-n junction where doped regions contain a-Si:H and the absorber layer is a a-Si:H and µc-Si mixture.

Figure 1 depicts the schematic of PI Energy's solar cell, highlighting the absorber layer grown on a laser annealed interface known as the seed layer. PI Energy aims to develop a pure crystalline silicon layer (epitaxial Si) measuring 1 micron in thickness, positioned between two a-Si:H layers. The company employs a low-temperature Plasma Enhanced Chemical Vapor Deposition (PECVD).

By laser annealing a seed layer on top of the n-type a-Si:H layer, PI Energy intends to create an ideal template for the growth of epitaxial crystalline silicon. Currently, the laser annealing process at PI Energy is suboptimal, resulting in seed layer films consisting of a mix of amorphous and crystalline silicon. The absorber layer is mostly a-Si:H.

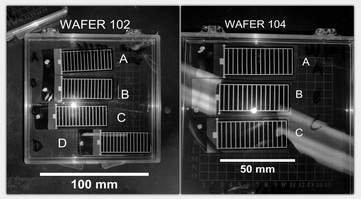

Fig 2. This image demonstrates wafer 102 and 104. These were used in SEM, Photoluminescence, and UV-Vis tests.

Methods

- **Atomic Force Microscopy (AFM)**
  Surface roughness measurements were taken with a Park Systems XE 7 AFM. A Park Systems SmartScan for XE collected data. Data was collected with an Opus 3XC-NA tip at a constant force of 0.3 N/m in contact mode. The purpose of this experiment was to look for correlations between relative laser energy and seed layer roughness of wafer 88.

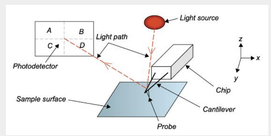

Fig 3. This image demonstrates a general AFM setup.

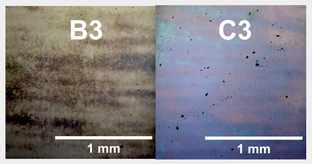

Fig 4. Optical Micrographs of Wafer 88

- **Optical Microscopy (OM)**
  Optical microscopy images were taken with a Liss Microsystems microscope and a Leica 1C1 Camera. Bulk differences on seed layers subjected to different relative laser annealing energy densities were imaged and analyzed. The purpose of this experiment was to look for correlations between relative laser energy and seed layer morphology.
- **Cross-sectional Scanning Electron Microscopy (SEM) with Focused Ion Beam (FIB) Milling**
  SEM micrographs were taken with a FEI Scios DualBeam FIB-SEM. FIB Milling was performed with an ion beam depth of 1.5 um. The purpose of this experiment was to compare the thickness of the film layers and morphology between wafers 102 (worse performing) and 104 (better performing).
- **Photoluminescence (PL)**
  Steady-state PL measurements were taken with a Vortran laser at a 532 nm excitation wavelength. Intensity was measured with a Princeton HRS-300 spectrophotometer and a Pixis 400 camera. Time-resolved PL measurements were taken with a Picoquant LDH-IB-450B laser source at a 457 nm excitation wavelength. PL intensity was measured with a Picoquant PMA Hybrid 50 detector. These experiments compared photovoltaic properties between wafer 102 and 104.
- **Ultraviolet-Visible Spectroscopy (UV-Vis)**
  UV-Vis spectroscopy was performed with a Thermo Scientific-Evolution 220 UV-Visible Spectrometer. Reflectance measurements were taken for wafers 88 and 89. The purpose of this experiment was to look for the relative sizes of crystalline silicon peaks in the photovoltaic.

Results

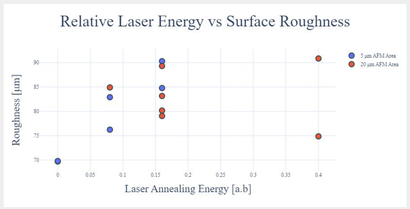

Fig 5. Surface roughness vs Relative Laser Energy Density data as collected using AFM.

AFM was performed on our first set of samples. Data was collected then analyzed using Gwyddion to find the surface roughness. **Figure 5** on the left shows the resulting surface roughness values in relation to the relative laser energy densities of the sample.

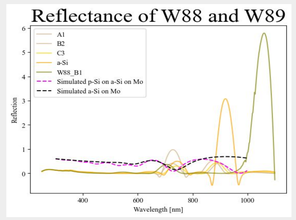

Fig 6. Graph of reflectances from wafer 88 and 89 alongside simulated a-Si/pc-Si samples.

UV-Vis spectroscopy data was collected for sample wafers 88 and 89. Data was compared to a theoretical model to gain a better understanding of the observed peaks. Factors used to predict the simulation were refractive index and film thickness of the photovoltaic. Experimental data was compared to the simulated data, demonstrated in **Figure 6**.

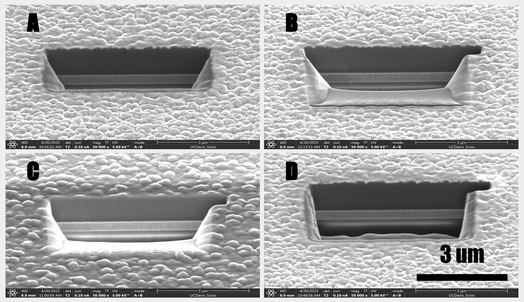

Fig 7. This image demonstrates micrographs from wafers 102 and 104. These were FIB milled and imaged by the SEM.

Wafer 102 performed worse than wafer 104 despite minor processing differences. In **Figure 7**, the various layers of the thin-film are visible. There are no obvious differences in the morphology of the four main samples. Using ImageJ, layer thickness was measured. We expected to see a crystalline silicon layer thickness difference between wafer 102 and 104, but rather saw a significant difference in thickness based on if the samples had been laser annealed or not.

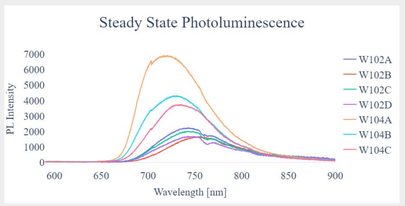

Fig 8. This demonstrates the steady state photoluminescence curves for wafers 102 and 104. Localized peaks at 700 nm were caused by the detector's shutter.

The emission spectra in **Figure 8** appears to be a gaussian distribution with a peak between 710 and 740 nm. This suggests all samples contained a majority a-Si:H. The double peaks for the wafer 102 may be caused by Shockley-Read-Hall recombination, resulting in the poorer performance.

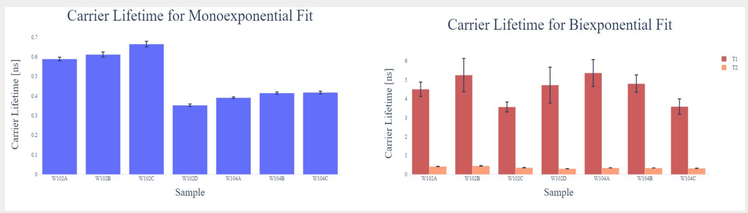

Fig 9. A biexponential and monoexponential curve fit were used on the time-resolved photoluminescence data. Neither fit appears to be more accurate than the other.

Time-resolved photoluminescence data was collected and fit to a monoexponential and biexponential curve with python. The monoexponential fit suggests a difference in carrier lifetime between wafer 102 and 104.

Discussion/Conclusion

AFM

- The results are inconclusive. While the 5 micron AFM area appears to demonstrate a slight linear trend between surface roughness and laser annealing energy, the 20 micron AFM area displays no trend.

OM

- Samples laser annealed at a lower relative laser energy density had a rougher morphology and greater surface damage.
- No correlation between relative laser energy density and morphology was found.

SEM

- No definitive conclusion on why there is a difference in performance between wafer 102 and 104.
- No relation between the laser energy and layer morphology.
- Laser annealing might be etching the crystalline silicon.

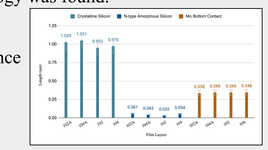

Fig 10. Layer Thickness vs. Annealing Condition

Steady-State PL

- Both wafers appear to be mostly a-Si:H, considering the peak intensity was 720 nm and the band gap of a-Si:H is 1.7 eV, matching the energy of photons at a 730 nm wavelength.
- Double peaks in the wafer 102 sample suggest Shockley-Read-Hall recombination.
- Wafer 104 had greater PL intensity than wafer 102, although the opposite was expected.

Time-Resolved PL

- The monoexponential fit suggests wafer 102 has a bulk carrier lifetime of 0.6 ns, while wafer 104 has a bulk carrier lifetime of 0.4 ns.
- The biexponential fit indicates no significant differences in bulk carrier lifetime between the wafers.
- Recombination mechanisms cannot be conclude from these graphs.

UV-Vis Spectroscopy

- The data demonstrates the sample is mostly amorphous
- Experimental data did not match with the simulated models; may be due to complexity in equipment and samples

Future Work

- Perform AFM analysis on more samples to get a general trend for the surface roughness effects with respect to laser annealing
- Use EBSD to analyze differences in crystallinity between the layers
- Determine whether Shockley-Read-Hall recombination accounts for the performance difference between wafer 102 and 104
- Fit TRPL data to $I=I_0\exp(-(t/\tau_1)^{\beta})$ curve (used for a-Si:H samples in literature)
- Fit the SSPL data to gaussian curves

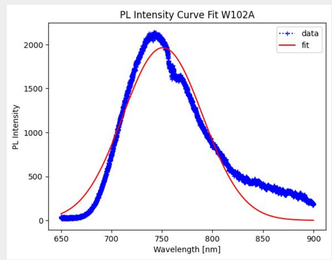

Figure 11. PL Intensity Curve Fit for Wafer 102

Acknowledgements

We would like to acknowledge: Amir Saeidi, Cassondra Brayfield, Edmund Dale, Hudson Shih, Seung Sae Hong, Mansha Dubey, Andrew Li, Sahar Daemi, and Ryan Anderson.

References

[1] R. A. Marques Lameirinhas, J. P. N. Torres, and J. P. De Melo Cunha, "A Photovoltaic Technology Review: History, Fundamentals and Applications," Energies, vol. 15, no. 5, p. 1823, Mar. 2022, doi: 10.3390/en15051823.

[2] R. E. I. Schropp, "Amorphous and Microcrystalline Silicon Solar Cells," in Solar Cell Materials, G. Conibeer and A. Willoughby, Eds., Chichester, UK: John Wiley & Sons, Ltd, 2014, pp. 85–111. doi: 10.1002/9781118695784.ch5.